

Characterization of Magnetite Scale Formed in Naphthenic Acid Corrosion

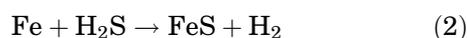
PENG JIN ^{1,2} WINSTON ROBBINS,¹ GHEORGHE BOTA,¹ and SRDJAN NESIC¹

1.—Department of Chemical and Biomolecular Engineering, Institute for Corrosion and Multiphase Technology, Ohio University, Athens, OH 45701, USA. 2.—e-mail: pj221108@ohio.edu

Naphthenic acid corrosion (NAC) is one of the major concerns for corrosion engineers in refineries. Traditionally, the iron sulfide (FeS) scale, formed when sulfur compounds in crudes corrode the metal, is expected to be protective and limit the NAC. Nevertheless, no relationship has been found between protectiveness and the characteristics of FeS scale. In this study, lab scale tests with model sulfur compounds and naphthenic acids replicated corrosive processes of refineries with real crude fractions behavior. The morphology and chemical composition of scales were analyzed with scanning electron microscopy and transmission electron microscopy. These high-resolution microscopy techniques revealed the presence of an iron oxide (Fe₃O₄ or magnetite) scale and discrete particulates on metal surfaces under FeS scales, especially on a low chrome steel. The presence of the iron oxide was correlated with the naphthenic acid activity during the experiments. It is postulated that the formation of the magnetite scale resulted from the decomposition of iron naphthenates at high temperatures. It is further postulated that a nano-particulate form of magnetite may be providing corrosion resistance.

INTRODUCTION

Naphthenic acid corrosion (NAC) is one of the major concerns for corrosion engineers in refineries.^{1,2} Increased processing heavy oils with high naphthenic acid content may lead to severe corrosion of facilities at temperatures from 240°C to 400°C. Sulfur compounds in crude oils also contribute to refinery corrosion at these temperatures. Crude oils vary widely in concentrations of naphthenic acids, commonly measured as total acid number (TAN, milligram of potassium hydroxide required to neutralize 1 g crude oil). Mixed sulfur and naphthenic acid (SNAP) corrosion is generally discussed in terms of the following reactions:³

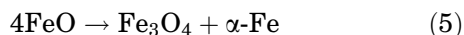
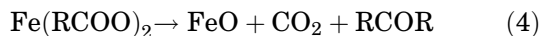


In Reaction 1, naphthenic acids are represented as RCOOH with R being a hydrocarbon structure and -COOH being the corrosive carboxylic group

that reacts with iron in the steel to form oil-soluble iron naphthenate (Fe(RCOO)₂). In Reaction 2, sulfur compounds in the crude oil, represented by hydrogen sulfide (H₂S), corrode the steel and form solid iron sulfide (FeS), which is not soluble in oil. This process is also known as sulfidation. Reaction 3 is not a corrosion reaction but two secondary reactions between the two primary corrosion products. In the forward reaction, hydrogen sulfide can react with iron naphthenate and regenerate naphthenic acids; in the reverse reaction, excess naphthenic acids can dissolve iron sulfide and release hydrogen sulfide.

In the refining industry, it is known that the iron sulfide forms a pseudo-protective scale on the steel surface that can deter SNAP corrosion, but conditions that affect the protective character of iron sulfide scales are not well understood.⁴⁻⁶ In our prior research, no correlation could be established between the corrosion resistance of scale and the concentration of naphthenic acids and sulfur compounds in the crude fractions.⁷⁻¹¹ More importantly, magnetite in oxide layers was identified in scales formed in corrosion by solutions containing acids

alone. Oxide layers were observed in and under an iron sulfide scale when both acids and sulfur compounds were present in the solution. It was hypothesized that magnetite was formed by secondary reactions of the iron naphthenate via Reactions 4 and 5:



Both reactions are well known outside corrosion research. Iron carboxylates thermally decompose (ketonize) to carbon dioxide, ketones, and iron oxide at temperatures above 250°C (Reaction 4). The iron oxide formed (wüstite, FeO) is unstable below 500°C and disproportionate to magnetite and α -iron (Reaction 5).^{12–14} The ketonization of metal carboxylate salts, including iron carboxylates, has been used for more than 100 years to synthesize ketones and nano-particles of magnetite (Fe₃O₄) that have a broad range of applications in the electronics and medical industries.^{15–19}

In our prior research, magnetite was formed at 316°C in the acid-alone solution by similar reactions, but the effect of temperature and sulfur compounds on its formation were not clear. In current research, corrosion for solutions containing both acids and sulfur compounds was investigated at different temperatures. Cross sections of corrosion product scales were examined for morphology with scanning electron microscopy (SEM) and transmission electron microscopy (TEM), and the elemental composition was studied by energy-dispersive x-ray spectroscopy (EDS). Magnetite was identified from its convergent beam electron diffraction (CBED) pattern in the TEM.

EXPERIMENT

Experimental Specimens

To assess the corrosion of the materials used in the field, two commonly used steels in refineries were selected for experimentation, i.e., the A106 carbon steel (CS) and the A182-F5 chrome steel (5Cr). (Their chemical composition is shown in Tables I and II in the Supplementary Materials.) Steel specimens were in the shape of rings with an inner diameter 70.43 mm, an outer diameter 81.76 mm, and a thickness 5 mm. Before experiments, each specimen was polished with 400- and 600-grit silicon-carbide paper in succession. Iso-propanol was used to flush specimens during polishing to prevent oxidation and overheating. After polishing, specimens were wiped with a paper towel, rinsed with toluene and acetone, and dried with nitrogen flow. The weights of fresh clean specimens were measured with an analytical balance.

After each experiment, specimens were rinsed with toluene and acetone, gently rubbed with a soft plastic brush, treated with “Clarke” solution (ASTM

G1 - 03), and reweighed. Based on the weight difference of specimens before and after the experiment and the exposed surface area, the corrosion rate was calculated.

Experimental Solutions

n-Dodecyl sulfide (DDS) and a commercial naphthenic acid mixture, denoted as “NAP” in the following text, were used to mimic natural sulfur compounds and naphthenic acids found in crude oil fractions. As in previous work,^{7–11} these reagents were dissolved in white mineral oil to prepare the solutions used to pretreat steel specimens. Three pretreatment solutions were prepared:

- “NAP only” consisting of NAP dissolved in mineral oil (TAN = 1.75, S = 0 wt.%)
- “DDS only” prepared of DDS dissolved in mineral oil (TAN = 0, S = 0.25 wt.%)
- “DDS + NAP” where both DDS and NAP were dissolved in mineral oil (TAN = 1.75, S = 0.25 wt.%)

The same NAP and mineral oil were used to prepare the corrosive TAN 3.5 solution used in the “challenge” experiment.

Experimental Equipment

As in previous work, two types of reactors were used in the experiment—a 1-L autoclave and a high-velocity rig (HVR).^{7–11} For pretreatment, six specimen rings (three of each alloy) were static (mounted on holder) and immersed in a stirred autoclave solution. For the challenge, specimen rings were mounted on a rotor inside the HVR reactor and rotated at 2000 rpm while the corrosive TAN 3.5 solution was continuously pumped through the reactor. The combination of once-through flow and rotational shear stress increased the severity of corrosion as discussed in our prior publications in which the scheme of the instrument was found.^{7–11}

Experimental Protocol

Although different temperatures and reactants were used to form the SNAP scales in the autoclave pretreatment, the resistance of the scale to acid attack was determined with the same temperature and higher concentration of acids.

Pretreatment

The 1-L autoclave was filled with 0.7 L of an experimental solution (“NAP only,” “DDS only,” or “DDS + NAP”) in which six steel specimens (three of each metallurgy) were immersed. Before the start of the experiment, the autoclave was flushed with nitrogen to remove oxygen, closed, and the temperature was raised to a preset value of 232°C, 316°C, or 343°C at which time the pretreatment started. After 24 h of pretreatment, the autoclave was cooled

to room temperature, opened, and the specimens were extracted for weight loss analysis and microscopic analysis.

To investigate the scale protectiveness, two parallel pretreatments were performed under the same condition. One set was used to determine the pretreatment corrosion rate by weight loss and characterization of the scale formed by microscopic analysis. The second set was used for the “challenge” as described as follows.

Challenge

Pretreated specimens with intact scales were extracted from the autoclave, mounted on the rotor, and installed in HVR. The HVR was fed with the corrosive TAN 3.5 solution flowing at 7.5 cm³/min, and the temperature was set to 343°C for 24 h. A back pressure of 1.1×10^6 Pa was applied to suppress the breakout of gas. The rotation of specimens produced a peripheral velocity of 8.5 m/s. The resistance of the SNAP scale to the acid attack was determined by weight loss.

Cuttings from pretreated specimens were mounted in epoxy and polished to expose the cross section for cross-section SEM analyses with a JEOL JSM-6390 SEM. Based on SEM results, selective specimens were analyzed by TEM on a Zeiss Libra 200EF TEM. Both SEM and TEM were equipped with an EDS detector to analyze the chemical composition. The crystal structure was determined by CBED analysis performed on TEM.

Corrosion Rate Calculations

The corrosion rates of specimens were calculated based on their weight loss during the experiment. For the *pretreatment* experiment conducted in the autoclave, the corrosion rate was calculated using Eq. 1. In a combined *pretreatment-challenge* experiment, freshly polished specimens were pretreated in the autoclave followed by challenging them in the HVR. The challenge corrosion was assessed using Eq. 2:

$$V_1 = \frac{87,600\Delta W_1}{\rho A_1 t} \quad (1)$$

$$V_2 = \frac{87,600(\Delta W_2 - \Delta W_1)}{\rho A_2 t} \quad (2)$$

In Eqs. 1 and 2, V_1 is the pretreatment corrosion rate, mm/y; V_2 is the challenge corrosion rate, mm/y; 87,600 is the unit conversion constant; ΔW_1 is the weight loss in the pretreatment step, g; ΔW_2 is the weight loss in the challenge step, g; ρ is the density of ring specimen, g/cm³; A_1 is the area of ring specimen exposed to pretreatment solution during the pretreatment, cm²; A_2 is the area of ring specimen exposed to corrosive TAN 3.5 solution during challenge, cm²; and t is the corrosion time, h.

RESULTS AND DISCUSSION

Pretreatment and Challenge Corrosion Rates

CS and 5Cr specimens showed similar *pretreatment* corrosion rates in each solution at each temperature (Fig. 1). In all three solutions, the corrosion rates increase with temperature with sulfidation by DDS only increasing more rapidly than acid corrosion by NAP only. With either single reactant, the 5Cr exhibited a lower corrosion rate than did the CS. The addition of DDS to NAP only appears to affect the combined corrosion rate at 343°C for both metallurgies. In other words, adding NAP to DDS seems to suppress sulfidation at the lower temperatures for both metallurgies. Nonetheless, NAP has a larger effect on sulfidation of CS relative to the 5Cr at 343°C. This suggests that chromium may be influencing the relative reaction rates of NAP and DDS with the iron in these two metallurgies.

The effect of chromium on the NAP corrosion with the two metallurgies can be observed in their “pure TAN 3.5 corrosion rates” in HVR (dotted lines in Fig. 2). These HVR corrosion rates are the values determined for freshly polished specimens with no surface pretreatment; i.e., these are the baseline for determining the resistance to the high-severity challenge. Because both metallurgies are in the same solution in each experiment, the four-fold difference in the challenge baselines can be compared with the two-fold difference in the pretreatment with acid at 343°C despite the difference in absolute concentrations (Fig. 1). This further indicates that chromium in 5Cr specimens is lowering the reaction rate of the iron in the steel with acids.

CS specimens pretreated in “NAP only” solution exhibited high-challenge corrosion rates close to the “pure TAN 3.5 corrosion rate.” That is, regardless of temperature, when pretreated with a lower concentration of NAP in the closed autoclave, challenge corrosion in the HVR continues unabated at the high-severity conditions with same acid. Similar results have been reported for these acids previously, but pretreatment with some model acids at 316°C have been shown to reduce corrosion rates in the challenge on CS.^{9–11} The differences among model acids and NAP were proposed to arise from differences in molecular structure.

The response of 5Cr specimens to “NAP only” pretreatment was strikingly different. Challenge corrosion rates were only ~50% of the baseline rate with pretreatment at 232°C and close to zero at 343°C, which is similar to the one with 316°C pretreatment previously reported. 5Cr specimens pretreated with the “NAP only” solution at lower and higher temperatures exhibited corrosion rates significantly below the “pure TAN 3.5 corrosion rates” (Fig. 2). In fact, at the two higher temperatures, the corrosion rate in the challenge is lower than the pretreatment at 343°C, further demonstrating that the NAP only pretreatment is changing the reaction mechanism on the 5Cr specimens.

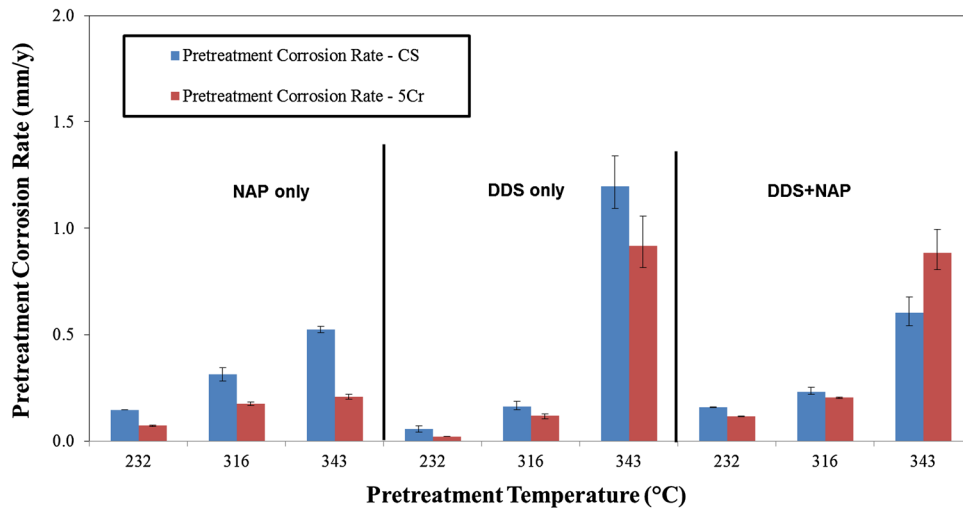


Fig. 1. Pretreatment corrosion rates of CS and 5Cr specimens at 232°C, 316°C, and 343°C.

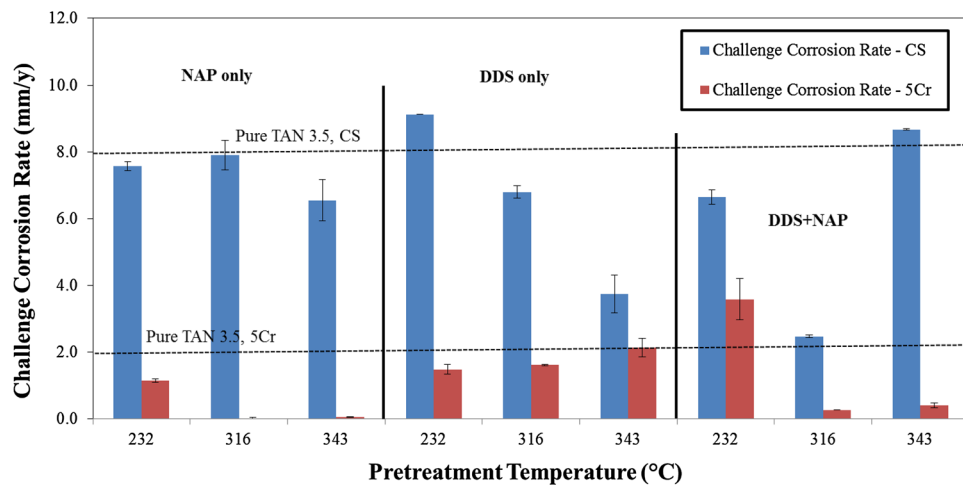


Fig. 2. Challenge corrosion rates for CS and 5Cr specimens pretreated with three solutions. Dotted lines indicate pure TAN 3.5 corrosion rates for CS and 5Cr specimens, respectively.

Additional differences are observed in the temperature response of CS and 5Cr specimens with the “DDS + NAP” solution. The challenge corrosion rates do not appear to relate directly to either of the single reagent solutions. At 232°C, the challenge corrosion rates were close to or above the corresponding “pure TAN 3.5 corrosion rate” in contrast to the previously reported reduced rates at 316°C (Fig. 2). Magnetite has been previously reported to contribute to resistance to acid corrosion for both CS and 5Cr specimens with this mixture at 316°C. Yet, when the pretreatment temperature was increased to 343°C, the corrosion rates for the two metallurgies diverged; corrosion resistance was lost on the CS specimen while it was retained for the 5Cr specimen. This may suggest that the chromium is facilitating magnetite formation in part by interfering with the competition for scale formation by sulfidation. Overall pretreatment temperatures

appear to have a larger effect on the surface reactions of DDS and NAP on 5Cr specimen than on CS specimen. Therefore, the following characterization of pretreated surfaces focuses on 5Cr specimens by TEM analysis. (Results of SEM analysis are included in the supplementary materials.)

TEM Analysis

The TEM images of 5Cr specimens pretreated in “NAP only” solution at the three temperatures were recorded at different resolutions (Fig. 3). The TEM image for the specimen pretreated at 232°C exhibits no scale on the steel surface. On the other hand, at higher magnification, TEM images show scales between the Pt coating and the base metal for the pretreatment at 316°C and 343°C. For the pretreatment at 343°C, the scale became thicker with larger grains.

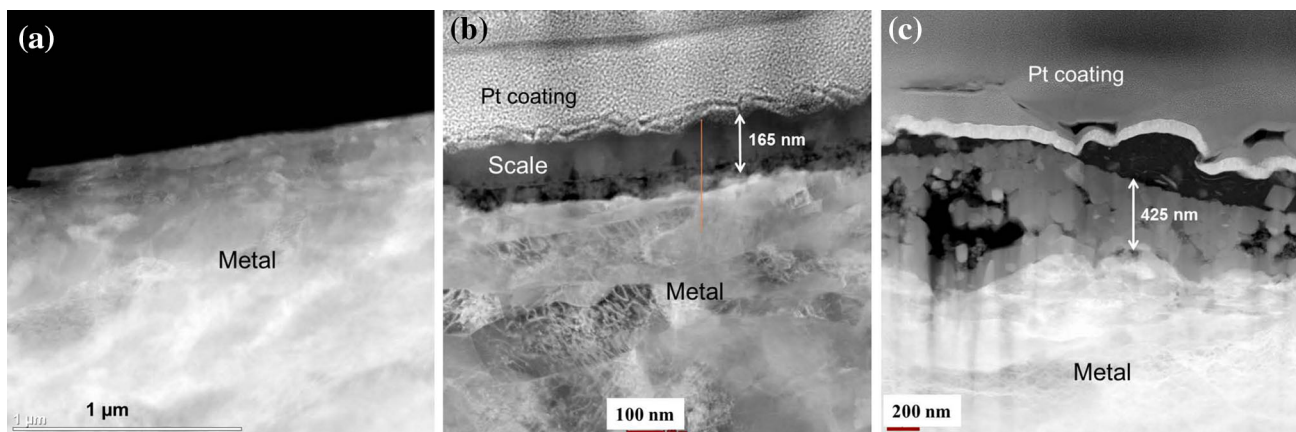


Fig. 3. TEM images of 5Cr steel specimens pretreated with “NAP only” solution (a) 232°C, (b) 316°C, and (c) 343°C.

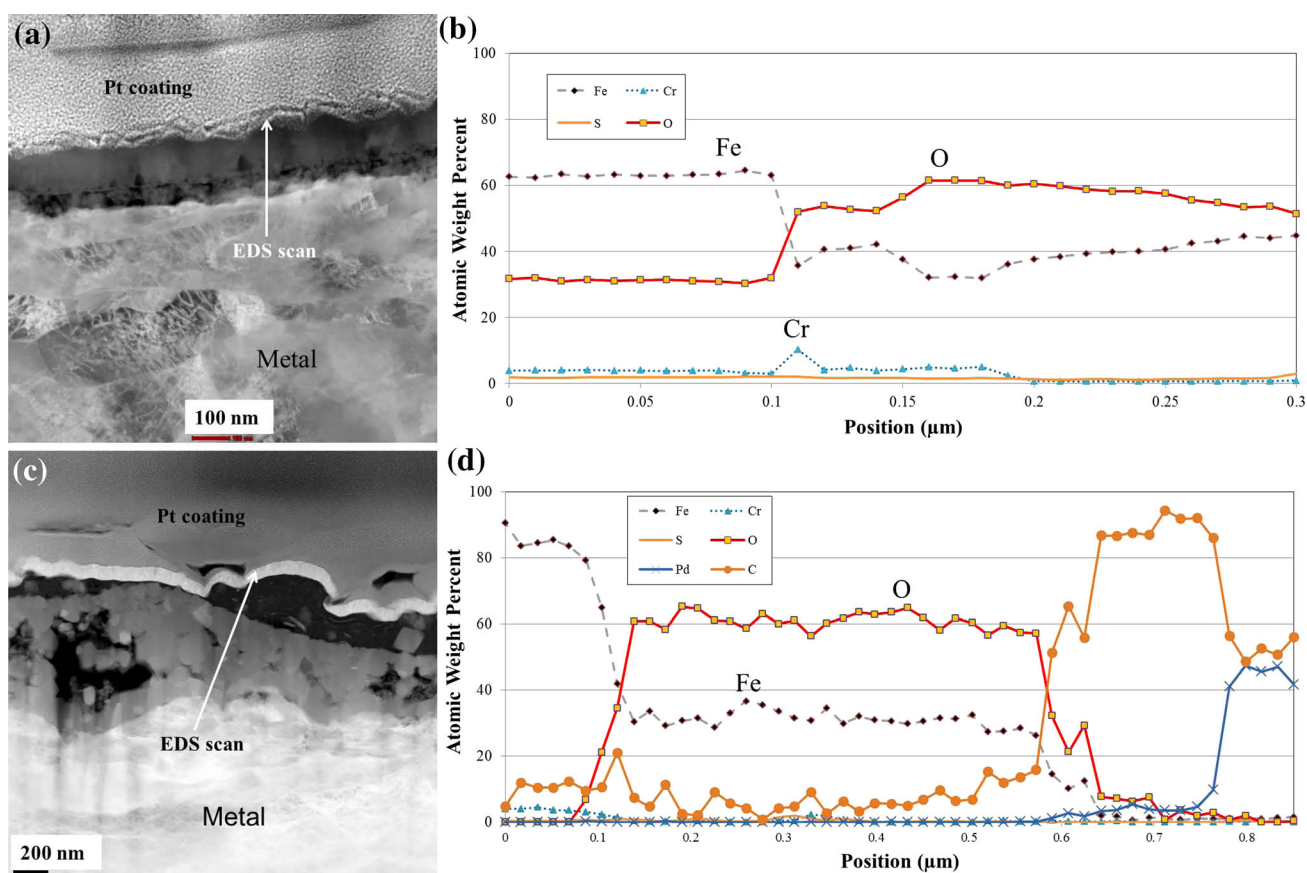


Fig. 4. TEM image and EDS analysis on the scale formed on 5Cr specimen pretreated with “NAP only” solution at 316°C (a and b) or 343°C (c and d). The elemental data were collected along the white line from the bottom to the top.

Figure 4 compares the TEM/EDS line analyses for 5Cr specimens pretreated with “NAP only” solution at 316°C and 343°C. For the scale formed at 316°C, the inner layer appears to contain about 5% chromium consistent with the base metal, whereas chromium is absent in the outer layer (Fig. 4a and b). In contrast, a higher O/Fe ratio (60/35) for the thicker scale formed in the 343°C pretreatment where “NAP only” solution

is found (Fig. 4c and d). Low concentrations (<2%) of sulfur at both temperatures could arise from trace sulfur contained in NAP and/or from the slight contamination of the autoclave.

CBED analysis for spots on the inner layers detects magnetite (Fe_3O_4) in the oxide scale formed in the pretreatment in “NAP only.” (See Fig. 3a in the supplementary materials.)

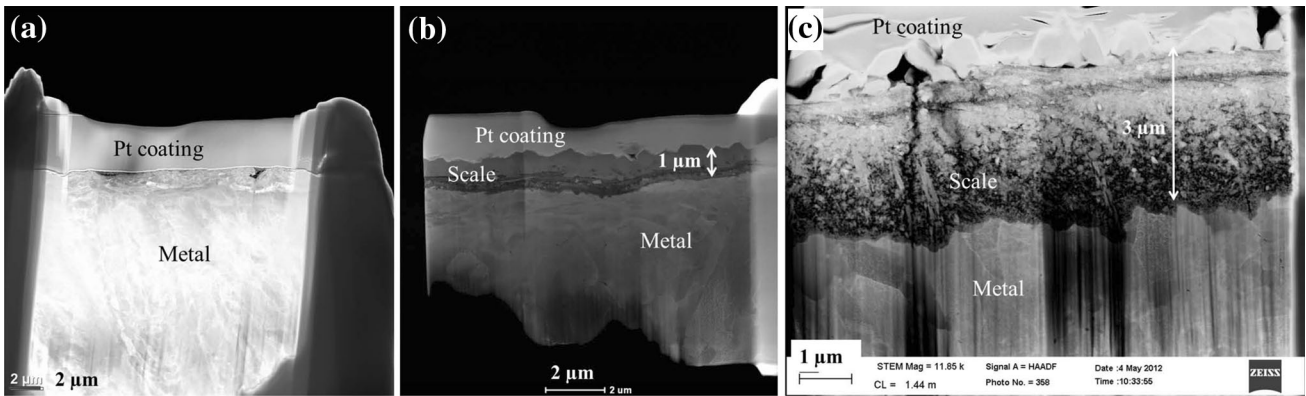


Fig. 5. TEM images of 5Cr steel specimens pretreated with “DDS + NAP” solution (a) 232°C, (b) 316°C, and (c) 343°C.

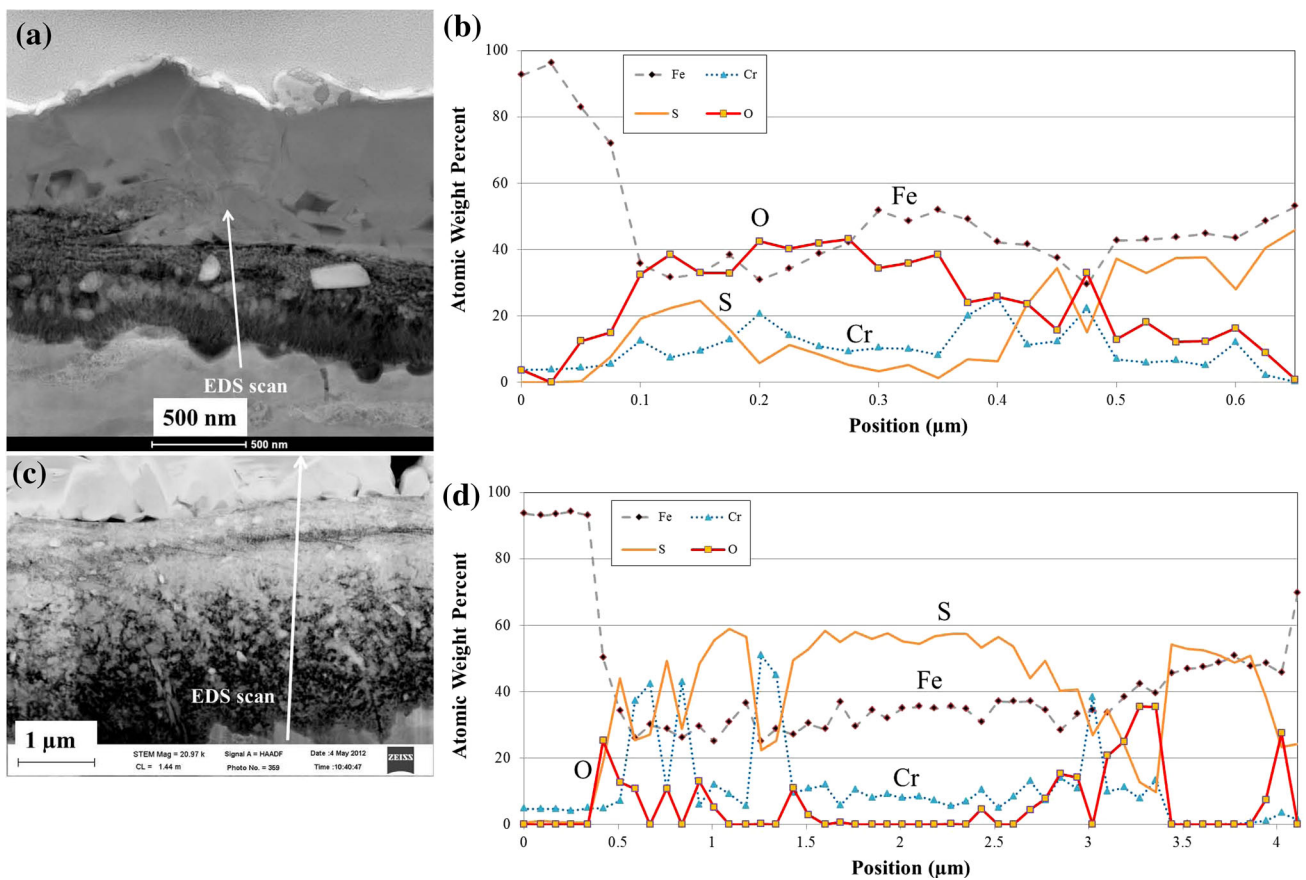


Fig. 6. TEM image and EDS analysis on the scale formed on 5Cr specimen pretreated with “DDS + NAP” solution at 316°C (a and b) or 343°C (c and d). The elemental data were collected along the white line from the bottom to the top.

TEM detected no distinct continuous scale on the 5Cr specimen pretreated with “DDS + NAP” at 232°C (Fig. 5a). On the other hand, TEM detected thicker scales after the pretreatment at 316°C and 343°C, respectively (Fig. 5b and c). The morphology of the scale formed at 316°C exhibits multiple layers, whereas a more complex fragmented scale is observed after pretreatment at 343°C.

The TEM/EDS line scan for the “DDS + NAP” pretreatment at 316°C indicates the presence of iron, chromium, oxygen, and sulfur at various ratios (Fig. 6a). In contrast to the results with “NAP only” pretreatment, the O/Fe ratio is lower with sulfur apparently making up the difference in anions. Furthermore, chromium is dispersed throughout the scale layers at atomic percentages higher than

the 5% in the steel. The scale formed at 343°C appears thicker with a much more fragmented morphology (Fig. 6c). EDS line analysis shows lower oxygen content than in the scale formed at the 316°C. With “DDS + NAP” pretreatment at 343°C, the inner region appears to consist of particulate iron and chromium oxide with a Fe/Cr/S intermediate layer capped with an iron oxide and then a final iron sulfide layer (Fig. 6d). Interestingly, the chromium concentrations spike up where oxygen and sulfur decrease in the highly fragmented lower regions of the scale.

DISCUSSION

In the challenge, the metal loss reflects corrosion resulting from diffusion of the acid through a scale to attack the metal substrate. Protective magnetite scales have been identified in “NAP only” pretreatment of 5Cr specimens at 316°C and 343°C. The granularity of the magnetite detected by TEM in scales suggests that nano-particulate magnetite is being formed in the pretreatment. Results of recent studies have shown that nano-particulate magnetite can be used to catalyze the ketonization of carboxylic acids.²⁰ Thus, once formed, these nano-particulates could serve to intercept and catalytically destroy acids before they can diffuse to the base metal to cause corrosion. Chromium appears to play a role in the formation of the nano-particulate. It may be facilitating the formation of discrete nano-particles. Findings from current research reveal that much remains to be learned about nucleation, aggregation, and particle size control in magnetite nano-particulate synthesis.²¹

The presence of the sulfur compound also affected the formation and properties of oxide scale. For the scale formed in the pretreatment in “DDS + NAP” at 316°C, particulate oxides are distributed within a chromium-enriched iron chromium sulfide particle. At 343°C, iron oxides are distributed above and below an oxygen-free Fe/Cr/S layer. These observations may be explained as follows: At 316°C, the reactive sulfur compound (DDS) competes with the acid for the iron and forms the iron sulfide layer.²² Naphthenic acid in the bulk fluid continues to diffuse through the sulfide layer on the steel surface and generates iron naphthenates. The iron naphthenates decompose to nano-particulate magnetite while the reactive sulfur forms the sulfide layer so that both reactions contribute to the formation of a porous structure. Given the large molecular size (twice of originating naphthenic acid), any iron naphthenate generated under the sulfide layer also contributes to the nano-particulate iron oxide. At 343°C, the kinetics of sulfidation are accelerated so that initial nano-particulates are distributed above and below the Fe/Cr/S sulfide. In both cases, where the nano-particulate oxides are present in a close metal surface, the acid challenge corrosion rates are low.

CONCLUSION

1. At 232°C, neither naphthenic acids nor DDS was corrosive and there was no significant amount of corrosion product formed in pretreatment with “NAP only,” “DDS only,” or “DDS + NAP” solution.
2. At higher temperatures (316°C and 343°C), iron sulfide scales were formed as a result of the sulfur content in pretreatment solutions, but no direct correlation could be found between sulfur content and the resistance to acid challenge.
3. Pretreatment with solutions containing NAP increased specimen resistance to NAC, especially for 5Cr steel.
4. Nano-particulate magnetite appears to be responsible for increased corrosion resistance of 5Cr specimens to NAC.
5. Chromium seems to facilitate the generation of nano-particulate magnetite from the thermal decomposition of iron naphthenates.

ACKNOWLEDGEMENTS

This work was supported by the Naphthenic Acid Corrosion Joint Industry Project (NAP JIP) at the Institute for Corrosion and Multiphase Technology, The Ohio University.

ELECTRONIC SUPPLEMENTARY MATERIAL

The online version of this article (doi:[10.1007/s11837-016-2164-y](https://doi.org/10.1007/s11837-016-2164-y)) contains supplementary material, which is available to authorized users.

REFERENCES

1. S.D. Kapusta, A. Ooms, A. Smith, F. Van den Berg, and W. Fort, *Proceedings of CORROSION/2004*, Paper no. 04637 (Houston, TX: NACE, 2004), p. 1.
2. G.Y. Lai, *JOM* 37, 14 (1985).
3. E. Slavcheva, B. Shone, and A. Turnbull, *Br. Corros. J.* 34, 125 (1999).
4. G.M. Bota and S. Nescic, *Proceedings of CORROSION/2013*, Paper no. 2512 (Orlando, FL: NACE 2013), p. 1.
5. V. Kanukuntla, D. Qu, S. Nescic, and A. Wolf, *Proceedings of CORROSION/2009*, Paper no. 2764 (Atlanta, GA: NACE 2009), p. 1.
6. Y. Yoon, I. Kosacki, and S. Srinivasan, *Proceedings of CORROSION/2016*, Paper no. 7598 (Vancouver, BC: NACE 2016), p. 1.
7. P. Jin, H.A. Wolf, and S. Nescic, *Surf. Interface Anal.* 47, 454 (2015).
8. P. Jin, W. Robbins, G. Bota, and S. Nescic, *Characterization of Minerals, Metals, and Materials 2016*, ed. D. Firrao, M. Zhang, Z. Peng, J.P. Escobedo-Diaz, and C. Bai (Nashville, TN: Wiley, 2016), p. 115.
9. P. Jin, W. Robbins, and G. Bota, *Proceedings of CORROSION/2016*, Paper no. 7302 (Vancouver, BC: NACE 2016), p. 1.
10. P. Jin, W. Robbins, and G. Bota, *Corros. Sci.* 111, 822 (2016).

11. P. Jin, G. Bota, W. Robbins, and S. Nestic, *Energy Fuel* 30, 6853 (2016).
12. S. Stolen, R. Gloeckner, and F. Gronvold, *Thermochim. Acta* 256, 91 (1995).
13. R. Chen, M.G. Christiansen, A. Sourakov, A. Mohr, Y. Matsumoto, S. Okada, A. Jasanoff, and P.O. Anikeeva, *Nano Lett.* 16, 1345 (2016).
14. C.J. Chen, R.K. Chiang, H.Y. Lai, and C.R. Lin, *J. Phys. Chem. C* 114, 4258 (2010).
15. E.R. Squibb, *J. Am. Chem. Soc.* 17, 187 (1895).
16. T.N. Pham, T. Sooknoi, S.P. Crossley, and D.E. Resasco, *ACS Catal.* 3, 2456 (2013).
17. M. Renz, *Eur. J. Org. Chem.* 2005, 979 (2005).
18. F.X. Redl, C.T. Black, G.C. Papaefthymiou, R.L. Sandstrom, M. Yin, H. Zeng, C.B. Murray, and S.P. O'Brien, *J. Am. Chem. Soc.* 126, 14583 (2004).
19. C.J. Chen, H.Y. Lai, C.C. Lin, J.S. Wang, and R.K. Chiang, *Nanoscale Res. Lett.* 4, 1343 (2009).
20. L.J. Gooßen, P. Mamone, and C. Oppel, *Adv. Synth. Catal.* 353, 57 (2011).
21. K.S.M. Salih, P. Mamone, G. Dörr, T.O. Bauer, A. Brodyanski, C. Wagner, M. Kopnarski, R.N.K. Taylor, S. Demeshko, F. Meyer, V. Schünemann, S. Ernst, L.J. Gooßen, and W.R. Thiel, *Chem. Mater.* 25, 1430 (2013).
22. J.A. Rodriguez, J. Dvorak, T. Jirsak, G. Liu, J. Hrbek, Y. Aray, and C. González, *J. Am. Chem. Soc.* 125, 276 (2003).